**Showcasing research from the groups of Prof. Haruo Inoue at Tokyo Metropolitan University and Prof. Yu Nabetani/ Prof. Tsutomu Shiragami at University of Miyazaki, Japan.**
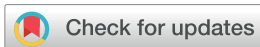
Heat trapping in a nano-layered microenvironment: estimation of temperature by thermal sensing molecules

An unusual heat-trapping within the nano-layered microenvironment composed of bilayer structured polyfluorinated cationic surfactants sandwiched by inorganic nano-sheets has been found. A dam-up effect on the dissipation of excess energy from the microenvironment surrounding the probe molecules is operating in the hybrid compounds, which rationalizes the previously observed unusually high quantum yield of photo-isomerization and the three-dimensional morphological motion of the hybrid compounds.

As featured in:
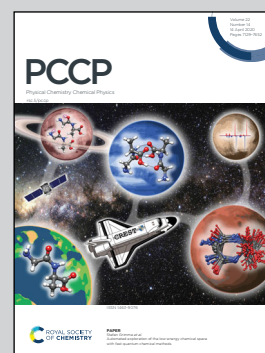
See Yu Nabetani, Haruo Inoue *et al*., *Phys. Chem. Chem. Phys*., 2020, **22**, 7201.

Check for updates

Heat trapping in a nano-layered microenvironment: estimation of temperature by thermal sensing molecules

Vivek Ramakrishnan, [iD] †[a] Yu Nabetani, [iD] *[b] Daisuke Yamamoto,[a] Hiroshi Tachibana[a] and Haruo Inoue [iD] *[a]

We have previously found reversible photo-induced expansion and contraction of organic/inorganic clay hybrids, and even sliding of niobate nano-sheets at the macroscopic level of organic/inorganic niobate hybrids, induced by the molecular photo-isomerization of the polyfluoroalkylated azobenzene derivative (**C3F-Azo-C6H**) intercalated within the interlayer, which is viewed as an artificial muscle model unit. Based on systematic investigations of the steady state photo-isomerization and transient behavior of the reaction, we comprehended that the phenomena is caused by trapping of excess energy liberated during the isomerization, as well as the relaxation processes upon excitation of azobenzene chromophores in the interlayers of the hybrid. In this paper, quantitative estimation of transient 'heat' trapped in various microenvironments has been studied by each co-intercalation of temperature sensing dye molecules – rhodamine B (RhB) or tris(bipyridine)ruthenium(II) chloride (Rubpy) with **C3F-Azo-C6H** within clay (SSA) nano-layers. The amount of dye molecules co-intercalated was kept to trace amounts that did not alter the bi-layered structure of the hybrid. The temperature of the microenvironment surrounding the probe molecules was estimated from the emission lifetime analysis. The evidently reduced emission lifetimes in **C3F-Azo-C6H**/SSA and **C3H-Azo-C6H**/SSA hybrids in the film state, indicated the elevation of temperature of the microenvironment upon excitation of the chromophores, which demonstrated our previous hypothesis rationalizing that the high reactivity of isomerization in the hybrid film state is caused by heat trapping *via* multi-step dissipation of the excess energy. With the hybrid of a hydrocarbon analogue (**C3H-Azo-C6H**), a distinct difference in temperature gradient was found to show the crucial role of the perfluoroalkyl chain of the surfactant that traps the excess energy to retard its dissipation leading to three-dimensional morphological motion.

1. Introduction

Based on the vastly accumulated chemical science knowledge of the molecular level, the frontiers of modern chemistry have been spreading their wings over the science of supramolecular systems, where molecular systems interact to provide unique microenvironments for chemical reactions and lead to the manifestation of specific functions.[1–6] The interactions of both attractive and repulsive forces act within the supramolecular systems, including electrostatic, hydrogen bonding, coordinating, hydrophilic, hydrophobic, and van der Waals *etc.*, which are often observed to operate simultaneously in many natural and bio-inspired human-made systems.[1–6] In addition to these, our research group has focused attention on other types of interaction – strong hydrophobicity and lipophobicity – exerted by perfluorinated compounds, which would be expected to be one of the key factors controlling the microstructure of supramolecular systems,[7–11] though not much attention has been paid to them so far. A solute molecule in a perfluorinated environment is known to behave like a molecule in the gas phase and thus the activity of solute molecules might be strongly affected when they are faced with, or doped in, the perfluorinated environment.[12–15] The almost non-existent immiscibility of the perfluoroalkyl group with both water and organic solvents, has been successfully solved by getting perfluoroalkyl groups and long hydrocarbon chains together, as both terminal ends of the ammonium-type cationic surfactants form supramolecular systems such as micelles,[3] reversed micelles,[7]

[a] Department of Applied Chemistry, Graduate School of Urban Environmental Sciences, Tokyo Metropolitan University, 1-1, Minami-ohsawa, Hachioji, Tokyo 192-0397, Japan. E-mail: inoue-haruo@tmu.ac.jp

[b] Department of Applied Chemistry, Faculty of Engineering, University of Miyazaki, 1-1, Gakuen-kibanadai-nishi, Miyazaki-shi, Miyazaki 889-2192, Japan. E-mail: yu.nabetani@cc.miyazaki-u.ac.jp

† Present address: National Solar Energy Centre, Ben-Gurion University of the Negev, Sede Boqer Campus, 84990 Israel.

This journal is © the Owner Societies 2020

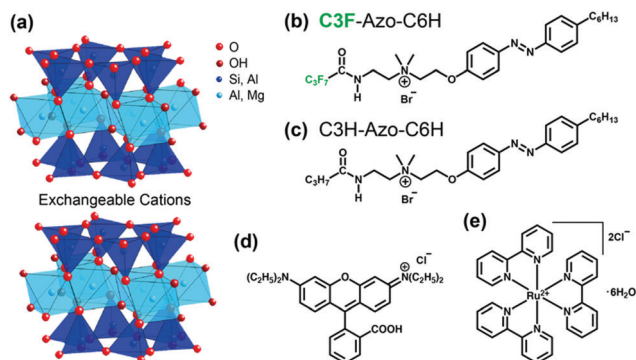*Phys. Chem. Chem. Phys.*, 2020, **22**, 7201–7209 | **7201**

Fig. 1 Crystal structure of (a) an inorganic layered clay mineral, Sumecton SA (SSA); chemical structures of: (b) polyfluorinated cationic surfactant (**C3F-Azo-C6H**), (c) alkylated cationic surfactant (**C3H-Azo-C6H**), (d) rhodamine B (RhB), and (e) tris(bipyridine)ruthenium(II) chloride (Rubpy). Fig. 1(a–c) were reproduced with permission from ref. 20, by permission of the Royal Society of Chemistry (2014).

vesicles,[8] and organic/inorganic hybrid compounds.[9–11,16–24] The perfluoroalkyl chains within the surfactant form their own phase in those supramolecular assemblies. Layered materials such as clay (Sumecton SA (SSA), Fig. 1a) and niobate nano-sheets can accommodate the polyfluorinated surfactants within their interlayer space through electrostatic interactions to form a bilayer structure of the surfactant, where a "forest of perfluoroalkyl chains" is formed.[10,11]

Among them, the hybrid systems formed by the polyfluorinated cationic surfactants having azobenzene moiety (**C3F-Azo-C6H**, Fig. 1b) attract particular interest as they respond to light irradiation through *trans-*/*cis*-isomerization.[16–20,22] Interestingly, **C3F-Azo-C6H**/niobate hybrids showed three-dimensional reversible photo-induced motion on a macroscopic level (~ 1.5 µm),[18,19,22] which is viewed as an artificial muscle model unit (Fig. 2).

Evidently, the *trans-*/*cis*-isomerization of azobenzene moiety serves as the trigger of the morphology change of the hybrids. It should be interesting to see how the trigger is transformed into the macroscopic morphological change, and to see what the subsequent processes following the isomerization are, and what the key factors controlling the phenomena are. Previously, we have reported that the *cis-* to *trans-* isomerization in a clay hybrid system (**C3F-Azo-C6H**/SSA) exhibited an extraordinarily

high reactivity with the quantum yield exceeding unity ($\Phi_{cis-trans} = 1.9$) in the film state.[20] Heat trapping within the interlayer of the clay hybrid was postulated to induce the high reactivity. The excess energy liberated during the primary processes of photo-isomerization, including vibrational relaxation and exoergic transformation from the *cis*-form into the *trans*-form (in femtoseconds to picoseconds time domain) could be trapped within the interlayer sandwiched by the bilayer perfluoroalkyl chains. The subsequent slow processes (nanoseconds to microseconds) due to a step-wise release of the trapped heat were further evidenced by a nanosecond laser flash photolysis study.[23] To gain deeper insight into what happens within the interlayer of hybrid compounds upon excitation of a photo-responsive chromophore, temperature sensing experiments are designed here for the clay hybrid systems. If the excess energy is trapped as heat within the interlayer of the hybrid, the temperature of the microenvironment surrounding the corresponding chromophore should increase, which could be monitored by temperature sensing molecules.

Rhodamine B (RhB, Fig. 1d) is a well-known molecule for sensing changes of temperature as it affects the fluorescence lifetime.[25–27] The fluorescence lifetime of RhB molecules is governed by the rotational motion around the diethylamino group, where activation energy and ease of rotation will decrease the lifetime of emission and thus it is a molecular indicator of temperature (Fig. 3a). Kitamura *et al.* reported the fluorescence lifetime of RhB diminishing from several nanoseconds to 500 picoseconds as the temperature increased up to 60 °C.[27]

Another candidate sensing molecule is tris(bipyridine)-ruthenium(II) chloride (Rubpy, Fig. 1e) which is well-known for its photo-redox catalytic properties, but is utilised here as a temperature sensing guest molecule owing to its reduction in emission lifetime when the surrounding temperature increases.[28–32] The emission from the ³MLCT state (Fig. 3b, k_0) competes with the thermally activated ³d–d level (k_d) to reduce its lifetime in the case of temperature elevation of the microenvironment surrounding the molecule.[30,31]

In this paper, the excited state emission decay behaviour of the dye molecules RhB and Rubpy, in various microenvironments – water, **C3F-Azo-C6H** in water (micelle), **C3F-Azo-C6H**/SSA (hybrid film), and the corresponding hydrocarbon analogue, **C3H-Azo-C6H**/SSA (hybrid film: Fig. 1c) – were systematically studied. The emission lifetimes were evidently diminished indicating a rapid elevation of temperature only in the microenvironment
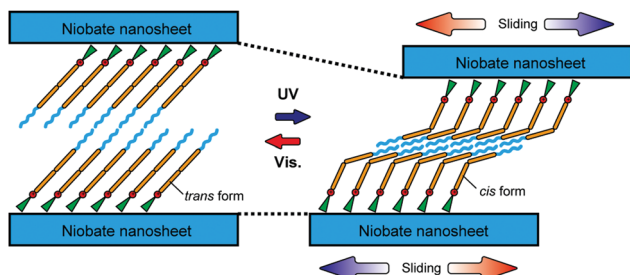

Fig. 2 Schematic diagram of the niobate nano-sheet sliding movement and interlayer distance change induced by photo-chemical *trans*–*cis* isomerization of the azobenzene molecules as an artificial muscle model unit.[18]
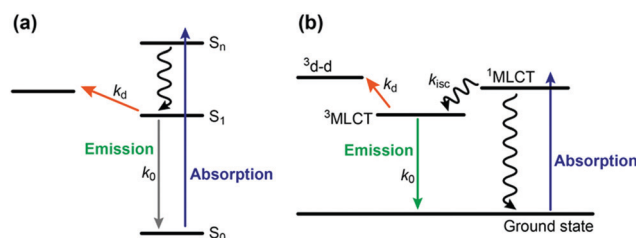

Fig. 3 Photo-physicochemical processes happening in: (a) RhB – fluorescence emission, and (b) Rubpy – MLCT mediated emission.

7202 | *Phys. Chem. Chem. Phys.*, 2020, **22**, 7201–7209

This journal is © the Owner Societies 2020

of hybrid compounds. The effect of the perfluoroalkyl chain was examined by comparing the behaviour with the case using the corresponding hydrocarbon analogue, **C3H-Azo-C6H** (Fig. 1c), to reveal more efficient heat trapping in the perfluorinated environment.

2. Results and discussion

2.1 Fluorescence decay dynamics of RhB and temperature estimation in various microenvironments

Upon selective excitation of the probe molecule (RhB) with visible light, the temperature elevation in the microscopic environment surrounding the probe molecule was estimated by observing how the fluorescence lifetime of RhB in the hybrid, **C3F-Azo-C6H**/SSA, was different from those in other environments such as water and **C3F-Azo-C6H** micelles. One of the most crucial points in designing experiments using a probe molecule should be to avoid an unexpected disordering/disturbing of the original microenvironment, thus RhB was here co-intercalated into the hybrid (**C3F-Azo-C6H**/SSA) in only 1% amounts *vs.* the cationic exchange capacity (CEC) of SSA with **C3F-Azo-C6H** of 440% (see Experimental). The X-ray diffraction (XRD) analysis of RhB-*co*-intercalated samples (RhB(1%)/**C3F-Azo-C6H**/SSA) proves that basal spacing (3.4 nm) is almost equivalent to the dye-free hybrids (3.2 nm).[19,20] With regards to the interlayer distance, the clay sample generally has a rather broad peak due to the small particle size of ~20 nm having inherent variation in the assignment of the peak top. According to our experience in preparing the organic/inorganic clay hybrid sample, we have judged that the interlayer distances among 3.4 nm and 3.2 nm for the hybrid with/without RhB(1%) are not altered. The absorption spectrum of RhB (500–550 nm) does not overlap with that of **C3F-Azo-C6H**, and the emission from RhB(1%)/**C3F-Azo-C6H**/SSA upon excitation at 540 nm is well characterized as the fluorescence of RhB itself (Fig. 4). Under the conditions in this study for the preparation of the film sample, the aqueous dispersion of SSA (1 g L^{-1}) has pH 9.93 after mixing with aerated water (pH 5.68). This is caused by the substitution of Na ions within the interlayer of the cationic exchange clay, with protons. The addition of the cationic ammonium surfactant (**C3F-Azo-C6H**) to the aqueous dispersion mixture, however, induced a reversion of the pH value down to pH 5.73 due to the complete substitution of the surface cation (proton) with the ammonium group of **C3F-Azo-C6H** intercalated within the interlayer under the conditions of CEC > 100%. In this study RhB (1% *vs.* CEC) is intercalated under the above condition of pH 5.73. RhB is well known to undergo protolysis at its carboxyl group with pK_a 3.22, and exhibits different fluorescence intensity under the lower/higher pH conditions corresponding to the pK_a, but the emission behavior is unaltered above pH 4 where RhB has a zwitterionic form with the dissociation of the carboxyl group.[33,34] The pH conditions in this study indicate that RhB has to be in the zwitterionic form in the interlayer of the clay to have stable fluorescent behavior.

In water at 22 °C, the fluorescence of RhB exhibited single exponential decay with a lifetime of 1.48 ns, which is well
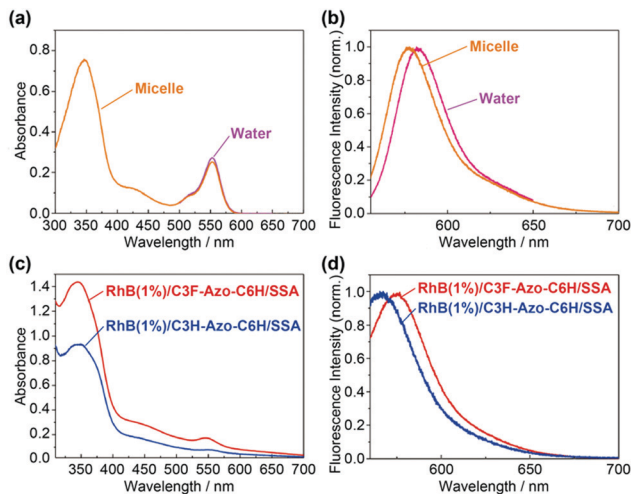

Fig. 4 (a) Absorption and (b) fluorescence spectra of RhB in solution state – water and **C3F-Azo-C6H**/water (micelle). (c) Absorption and (d) fluorescence spectra of RhB in the film state – RhB(1%)/**C3F-Azo-C6H**/SSA and RhB(1%)/**C3H-Azo-C6H**/SSA.

matched with the reported data.[25,27] RhB/**C3F-Azo-C6H**/water (micelle) showed also a single exponential decay of fluorescence with almost the same lifetime of 1.47 ns (Fig. 5). Contrary to the decay characteristics in water and micelle environments, the fluorescence of RhB in the RhB(1%)/**C3F-Azo-C6H**/SSA hybrid film exhibited non-single exponential decay, obeying bi-exponential decay with much shorter lifetimes of 0.17 and 0.73 ns compared to 1.48 ns in water (Fig. 5 and Table 1). The evident shortening of fluorescence lifetime surely indicates that the temperature of the microenvironment surrounding RhB in the hybrid compound is elevated upon selective excitation of RhB at 540 nm. This is in accordance with the expectation when designing the experiments as mentioned above.
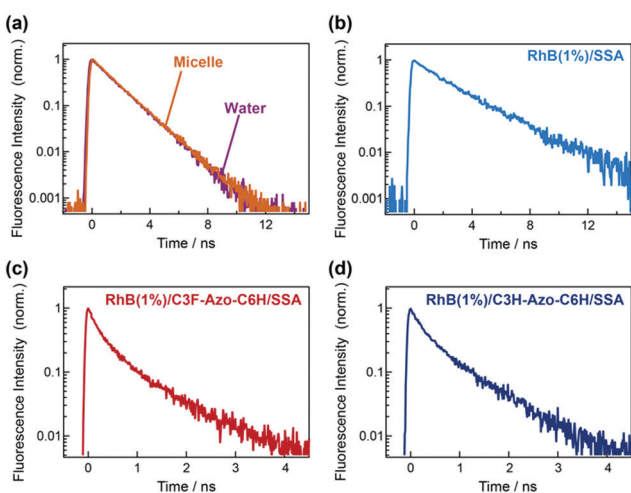
Fig. 5 Fluorescence decay of RhB in: (a) solution – water and **C3F-Azo-C6H**/water (micelle), (b) film state – RhB(1%)/SSA, (c) film state – RhB(1%)/**C3F-Azo-C6H**/SSA (all *trans*), (d) film state – RhB(1%)/**C3H-Azo-C6H**/SSA (all *trans*). Excitation at 540 nm (<0.25 μJ mm^{-2} under single photon counting conditions for the streak camera (Hamamatsu photonics, C4334)).

This journal is © the Owner Societies 2020

Phys. Chem. Chem. Phys., 2020, **22**, 7201–7209 | **7203**

Since **C3F-Azo-C6H** in an all *trans* form has almost no absorption at 540 nm, the temperature elevation should come from the retardational effect of the hybrid microenvironment on the dissipation of excess energy liberated during the vibrational relaxation and non-radiative processes, except the fluorescent one in the excited state of RhB. When two RhB molecules are in proximity forming a dimer, however, substantial electronic interaction causes a shortening of the lifetime down to 100 ps.[35,36] To check this possibility, RhB was solely intercalated in the interlayer of SSA in amounts of 1% *vs.* CEC (RhB(1%)/SSA) without **C3F-Azo-C6H** that is equal to the case of **C3F-Azo-C6H** (RhB(1%)/**C3F-Azo-C6H**/SSA). The fluorescence from RhB(1%)/SSA exhibits a single exponential decay with a lifetime of 2.24 ns (Fig. 5b and Table 1). This clearly indicates that RhB situates in the interlayer as a monomer without forming a dimer. The estimated temperature from the lifetime is, however, 5 °C (Table 1) that is rather lower than anticipated. The reason of the low temperature is not necessarily clear at present, but the estimation would not be simply caused by the temperature of the microenvironment surrounding RhB but also governed by the restricted environment for RhB in SSA without surfactant. The small interlayer distance for RhB(1%)/SSA (1.5 nm) implies that RhB situates in the more restricted environment in RhB(1%)/SSA than in fluid water where the calibration graph was made. Since the temperature estimation is based on the rotational motion of diethylamino substituent, the restricted motion in RhB(1%)/SSA might lead to the longer lifetime of the fluorescence corresponding to the apparently lower temperature than the real one in a normal motion in fluid water. Supposing a statistical distribution of RhB (1% *vs.* CEC) on the surface of SSA, where one anionic site for cation adsorption has 1.25 nm^2 as a hexagonal unit, each RhB (1% *vs.* CEC) has 125 nm^2 for its own occupation area, that is, the mean distance between each monomeric RhB is calculated to be 12 nm, which is sufficiently long to prevent almost all electronic interactions with each other. The distribution of RhB in RhB(1%)/**C3F-Azo-C6H**/SSA would be similarly statistical with that in RhB(1%)/SSA.

These experimental results and considerations thus led us to the conclusion that the bi-exponential fluorescence decay of RhB(1%)/**C3F-Azo-C6H**/SSA would reflect two kinds of RhB differently incorporated within the bilayer structure of **C3F-Azo-C6H**/SSA, but would not be due to distributions monomer and dimer forms of RhB.

Based on the report by Kitamura *et al.*,[27] the temperature elevation within the nano-layered microenvironment for both components can be estimated by eqn (1) that is rearranged as (2).

$$\tau^{-1} = k_0 + k_d = k_0 + A\exp(-\Delta E^{\ddagger}/RT) \qquad (1)$$

$$T = -\frac{\Delta E^{\ddagger}}{R}\cdot\frac{1}{\ln\dfrac{\tau^{-1} - k_0}{A}} \qquad (2)$$

where τ and k_0 (2.1×10^8 S^{-1}) denote the lifetime of the fluorescence of RhB and the rate constant of deactivation from the S$_1$ state, respectively, except the temperature dependent process, k_d. $\Delta E^{\ddagger}$ (2.8×10^4 J mol^{-1}) represents the activation energy for the process k_d; A (4.3×10^{13}) is the Arrhenius pre-exponential factor for k_d; R (8.314 J mol^{-1} K^{-1}) is the universal gas constant, respectively.

The temperature estimation from the fluorescence decay analysis shows pretty high temperature with gradients in the hybrid environment, while RhB in water and even in micelle conditions experiences no elevation of temperature from that of the experimental room (295 K, 22 °C), owing to very efficient and rapid dissipation of excess energy to the surrounding media (Table 1). The two component-decay of the fluorescence of RhB in hybrid environments suggests that RhB situates at two different microenvironments within the interlayer of the hybrid compounds. In RhB(1%)/**C3F-Azo-C6H**/SSA (all *trans*), species 1 suffered a higher temperature of 104 °C and species 2 was at 47 °C. With the **C3H-Azo-C6H** hybrid (RhB(1%)/**C3H-Azo-C6H**/SSA (all *trans*)) having longer fluorescence lifetimes, the lower value of temperature were estimated to be 89 °C and 40 °C (species 1′ and 2′, respectively), and compared with the polyfluoroalkylated environment (RhB(1%)/**C3F-Azo-C6H**/SSA (all *trans*)), this indicates that the dissipation of excess energy is more efficiently retarded in the polyfluorinated environment than in the corresponding hydrocarbon analogue. This is well in line with the previous observation in laser flash photolysis experiments.[23]

2.2 Emission decay dynamics of Rubpy and temperature estimation in various microenvironments

Another temperature probing molecule was further examined. Rubpy was chosen as the second probe that can monitor the more delayed time domain within several hundred ns by means of the spin-forbidden emission from the ^{3}MLCT state to the ground state, compared to the earlier temperature difference, within several ns for RhB, from the spin-allowed emission of the S$_1$ state. Fig. 6a and b show the absorption and emission spectra of Rubpy in water (λ_{max} = 454 and 606 nm) and Rubpy/**C3F-Azo-C6H**/water (micelle)

Table 1 Fluorescence decay lifetime and estimated temperature of RhB in various microenvironments

Microenvironment	Lifetime τ_1/ns	Temperature for τ_1/K	Lifetime τ_2/ns	Temperature for τ_2/K
RhB/water	1.48	295 (22 °C)	—	—
RhB/**C3F-Azo-C6H**/water (micelle)	1.47	295 (22 °C)	—	—
RhB(1%)/SSA	2.24	278 (5 °C)	—	—
RhB(1%)/**C3F-Azo-C6H**/SSA (all *trans*)	0.17 (0.61)^a	377 (104 °C)	0.73 (0.39)^a	320 (47 °C)
RhB(1%)/**C3H-Azo-C6H**/SSA (all *trans*)	0.24 (0.61)^a	362 (89 °C)	0.88 (0.39)^a	313 (40 °C)

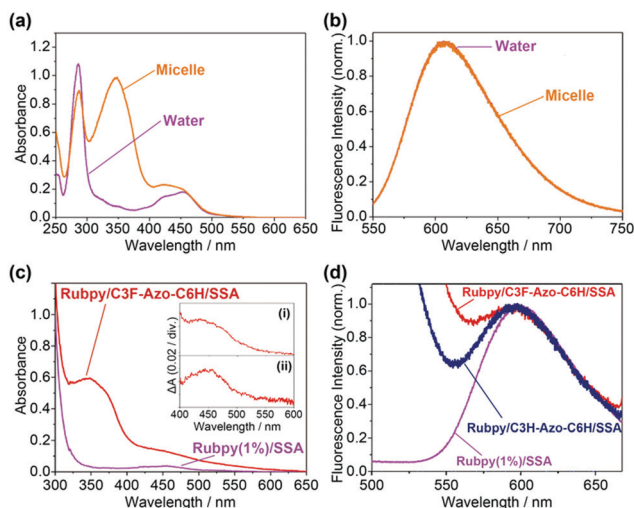^{a} Pre-exponential factor for the bi-exponential decay.

Fig. 6 (a) Absorption and (b) emission spectra of Rubpy in solution state – water, and **C3F-Azo-C6H**/water (micelle). (c) Absorption and (d) emission spectra of Rubpy in the film state – Rubpy(1%)/SSA, Rubpy/**C3F-Azo-C6H**/SSA, and Rubpy/**C3H-Azo-C6H**/SSA. The inset in (c) shows: (i) the difference absorption spectrum between Rubpy/**C3F-Azo-C6H**/SSA and **C3F-Azo-C6H**/SSA, (ii) the magnified absorption spectrum of Rubpy(1%)/SSA.
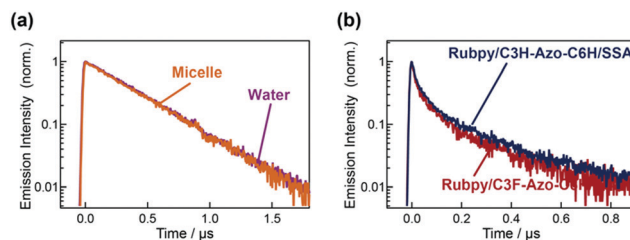

Fig. 7 Emission decay of Rubpy in (a) solution – water and micelle, (b) in the film state – Rubpy/**C3F-Azo-C6H**/SSA (all *trans*) and Rubpy/**C3H-Azo-C6H**/SSA (all *trans*). Excitation at 450 nm (< 0.25 μJ mm^{-2} under the single photon counting condition for the streak camera (Hamamatsu photonics, C4334)).

($\lambda_{\max}$ = ~450 nm and ~600 nm). Though the absorption peak of Rubpy (MLCT: t_{2g} of Ru to $\pi^{\star}$ of bipyridyl moiety) partly overlaps with n–$\pi^{\star}$ transition of **C3F-Azo-C6H** in the micellar system, excitation at 450 nm induced emission at ~600 nm that is characteristic of the ^{3}MLCT of Rubpy. Contrary to the case of RhB, the incorporation of Rubpy into the interlayer of the hybrid films (**C3F-Azo-C6H**/SSA and **C3H-Azo-C6H**/SSA) was not as feasible. With amounts of 1%, 2%, 5%, 10%, and 50% of Rubpy (*vs.* CEC of SSA) in water (loading level), co-intercalation was not observed when monitored by emission spectroscopy. With 100% loading level of dye, however, the co-intercalation was found to proceed.

The emission from the co-intercalated hybrid upon excitation at 450 nm was confirmed to be derived from Rubpy, but the intensity and the absorbance compared to those of Rubpy(1%)/SSA without surfactant, clearly indicates that the amount of Rubpy co-intercalated is lower than 1% *vs.* CEC even though the loading level is 100% (Fig. 6c(i) and (ii)). This could be due to the lower affinity of Rubpy against the negatively charged surface of SSA; Rubpy has the longer distance between the cationic Ru ion and the negative charge of the SSA surface because the Ru ion is situated in the centre of the Rubpy complex and is a bit apart from the molecular surface. In the case of RhB, however, the cationic ammonium group of RhB can directly face the surface of SSA to have a stronger affinity than Rubpy. Following this, we conducted the excited state lifetime measurements. Rubpy in water and Rubpy/**C3F-Azo-C6H**/water (micelle) exhibited the decay characteristic emission of Rubpy at around 600 nm in a single exponential manner (Fig. 7), as was similarly observed in the case of RhB. The lifetime of the emissions in both systems are comparable (390 ns in water and 380 ns in micelle). These are very close to the reported value of 400 ns in water,[29] indicating that the microenvironment

surrounding the Rubpy in a micelle (Rubpy/**C3F-Azo-C6H**/water) has not suffered a temperature change upon excitation of Rubpy as in fluid water, where energy dissipation is very efficient. In the hybrid compounds (Rubpy/**C3F-Azo-C6H**/SSA and Rubpy/**C3H-Azo-C6H**/SSA), however, the emission lifetimes substantially decreased with two-component decay as shown in Fig. 7 and Table 2. The two-component decays indicate again that Rubpy behaves as two kinds of species having different lifetimes, *i.e.*, it situates at two different sites within the interlayer of the hybrid compounds.

For Rubpy, emission is originally from the ^{3}MLCT at room temperature, and any elevation of temperature would enhance the excited state pumping to ^{3}d–d from ^{3}MLCT as Meyer and co-workers reported.[28,29] The "molecular heat" evolved by the radiationless deactivation process from the Franck–Condon excited state to the relaxed emissive state upon excitation of Rubpy, would be trapped within the surfactant/SSA layer and thus promotes the transition from ^{3}MLCT to ^{3}d–d to decrease the emission intensity from ^{3}MLCT. The effect of temperature on the kinetics is expressed in the same equations as eqn (1) and eqn (2) as applied for the case of RhB. In the equations, $\Delta E^{\ddagger}$ (4.82×10^4 J mol^{-1}) is the energy gap interpreted as the activation barrier for the ^{3}MLCT to ^{3}d–d state conversion, A (2×10^{14} s^{-1}) is the rate of barrier crossing, and k_0 (5×10^5 s^{-1}) is the Boltzmann averaged value of the decay rate constants from the three lower-lying MLCT states.[28,29] In Rubpy/**C3F-Azo-C6H**/SSA (all *trans*-form for azobenzene moiety) system, temperature calculations using eqn (2) for component 1 (τ_1) upon excitation of Rubpy gave the value of approximately 392 K (119 °C), and component 2 (τ_2) had the value of 342 K (69 °C). For the Rubpy/**C3H-Azo-C6H**/SSA hybrid system, the lifetimes of both components were found to be slightly longer, *i.e.*, lower temperature rise (385 K (112 °C) and 338 K (65 °C)) than the polyfluorinated hybrid film (Rubpy/**C3F-Azo-C6H**/SSA). Though the temperature estimation using Rubpy apparently affords a slightly higher value than the actual temperature as observed in Rubpy/water (315 K (42 °C)) that should be around 22 °C, the higher temperature elevation in Rubpy/**C3F-Azo-C6H**/SSA compared to Rubpy/**C3H-Azo-C6H**/SSA is again well in-line with our previous results that the perfluoroalkyl chain layer in the **C3F-Azo-C6H**/SSA hybrid has less intermolecular interaction to delay the dissipation of trapped thermal energy.[20,23]

This journal is © the Owner Societies 2020

Phys. Chem. Chem. Phys., 2020, **22**, 7201–7209 | **7205**

Table 2 Emission decay lifetime and estimated temperature of Rubpy in various microenvironments

Microenvironment	Lifetime τ_1/ns	Temperature for τ_1/K	Lifetime τ_2/ns	Temperature for τ_2/K
Rubpy/water	390	315 (42 °C)	—	—
Rubpy/**C3F-Azo-C6H**/water (micelle)	380	316 (43 °C)	—	—
Rubpy/**C3F-Azo-C6H**/SSA (all *trans*)	14 (0.64)[a]	392 (119 °C)	124 (0.30)	342 (69 °C)
Rubpy/**C3H-Azo-C6H**/SSA (all *trans*)	18 (0.65)[a]	385 (112 °C)	150 (0.31)[a]	338 (65 °C)

[a] Pre-exponential factor for the bi-exponential decay.

2.3 Effect of the polyfluorinated microenvironment on energy dissipation

According to the prediction that the polyfluorinated microenvironment in the layered hybrid compound could retard a random and rapid dissipation of excess energy liberated within the interlayer, just like a dam for excess energy,[23] it was expected that the temperature of the microenvironment would be elevated upon excitation of chromophores in the interlayer. Probing the temperature by means of two different molecules, RhB and Rubpy, has actually exhibited the substantial decrease of their emission lifetimes to demonstrate the temperature elevation of the microenvironment surrounding them upon excitation to their excited state (Table 1 and 2). Upon judging the soundness of experimental results obtained, a crucial point should be clarified here. An important questions is whether or not the trapped heat upon excitation of the dye molecule within the interlayer could interfere with the adjacent dye in the same interlayer, *i.e.*, is there any possibility of simultaneous excitation of the nearest two RhB* or Rubpy* within the same interlayer within the laser pulse and any mutual interference by propagation from other high temperature sites? The experiments here have carefully been designed to avoid the above possibility under the single photon counting condition for the laser pulse intensity below 0.25 µJ mm^{-2} (= 2.5×10^{-19} J nm^{-2}) to excite RhB at 540 nm or Rubpy at 450 nm. The probability of excitation of RhB or Rubpy by the pico second laser pulse (26 ps) was estimated using the cross section of light absorption by RhB (1.75×10^{-2} nm^2) or Rubpy (2.43×10^{-3} nm^2), both calculated by the extinction coefficient of RhB at 540 nm (1.05×10^5 M^{-1} cm^{-1}) or Rubpy at 450 nm (1.46×10^4 M^{-1} cm^{-1}), and the number of photons of the laser pulse per nm^2 at 540 nm (2.5×10^{-19} J nm^{-2}/220 kJ mol^{-1}: 0.68 nm^{-2}) for RhB, or 450 nm (2.5×10^{-19} J nm^{-2}/265 kJ mol^{-1}: 0.57 nm^{-2}) for Rubpy. Since the mean number of dye molecules incorporated into one SSA interlayer is calculated to be 6.4 from the size of SSA (top and bottom surfaces, ~800 nm^2), and the occupation area of the dye (at 1% *vs.* CEC, 125 nm^2), the probability of excitation of at least one RhB or Rubpy becomes 7.7% or 0.90%, respectively. The simultaneous excitation of two RhB or Rubpy within the same interlayer thus has only a probability of 0.50% or 0.0068%, respectively. In both cases the simultaneous excitation of RhB or Rubpy within the laser pulse duration is thus almost negligible. Since the laser is pulsed every 1 ms (1 kHz), the trapped heat upon excitation of RhB or Rubpy within the interlayer of the hybrid should completely dissipate during the next excitation after 1 ms. The experimental conditions adopted here thus assure a sound

observation of the temperature elevation and the heat dissipation within the interlayer of the hybrid microenvironment.

Among the two probe molecules, RhB was excited at 540 nm (220 kJ mol^{-1}) to fluoresce at around 583 nm (204 kJ mol^{-1}), where the amount of excess energy liberated through the rapid relaxation from the Franck–Condon excited state down to the relaxed fluorescent state is ~16 kJ mol^{-1}. It corresponds to *ca.* 4000 K in terms of the excess energy localizing only in a single mode degree of freedom ($kT/2$). For Rubpy, the excitation wavelength (450 nm: 265 kJ mol^{-1}) and the emission maximum (~600 nm: 199 kJ mol^{-1}) indicate the excess energy input would be ~66 kJ mol^{-1}, which corresponds to *ca.* 16 000 K for a single mode degree of freedom. Within several picoseconds the excess energy under such a high temperature would be rapidly shared among several modes of molecular motion; at first within the corresponding molecule and subsequently outside of the molecule including the microenvironment in the form of rotation, translation, vibration, *etc.*, to dissipate in a random manner and to cool down until thermodynamic equilibrium is reached.[37,38] The dissipation of excess energy is largely dependent on intermolecular interactions that are much stronger in ordinary fluid solution such as water and thus the cool down processes (equilibration) are very rapid, within several picoseconds.[37,38] On the other hand, those intermolecular interactions in the polyfluorinated microenvironment would be expected to be weak enough to retard the energy dissipation within the interlayer of the hybrid compound (**C3F-Azo-C6H**/SSA) as an exceptional case. Though the thermal conductivity of bulk liquid perfluorohexane (5.6×10^{-3} W m^{-1} K^{-1}) is much less than that of water (0.606 W m^{-1} K^{-1}), the surprisingly big difference of heat dissipation between water and the **C3F-Azo-C6H**/SSA hybrid environment is very curious and might be due to the specific microscopic environment of the interlayer, where each polyfluorinated cationic surfactant is strongly bound to the anionic site on the surface of SSA, and a convective heat transfer by translational motion of molecules should be mostly negligible. In the hybrid interlayer the perfluoroalkyl, ammonium, alkyl, and aromatic groups form a microenvironment with an ordered alignment, but a conductive heat transfer including intermolecular vibrational interaction and a radiative heat transfer at high temperature, might not be passed straightforwardly. Probing the degree of retardation of energy dissipation should be very interesting. Though probing the time constants of the retardational effect would not be so readily attainable, the estimation of temperature in a specific time domain would be possible to be probed. Since the lifetime of fluorescence of RhB in water is ~1.5 ns (Table 1), we can

7206 | *Phys. Chem. Chem. Phys.*, 2020, **22**, 7201–7209

This journal is © the Owner Societies 2020

probe the dissipation process of excess energy within $\sim$1.5 ns in terms of the "temperature" of the microenvironment, while Rubpy can probe it in a delayed time domain within $\sim$390 ns (Table 2). As the initial energy deposition upon excitation of chromophores is pretty different among RhB ($\sim$16 kJ mol^{-1}) and Rubpy ($\sim$66 kJ mol^{-1}), the temperatures estimated by the two probe molecules can not be straightforwardly compared. The evident elevation of temperature, however, in the hybrid compounds (**C3F-Azo-C6H**/SSA and **C3H-Azo-C6H**/SSA) when compared with the fluid water or even with the micellar environment, definitely indicates that the dam-effect on the dissipation of excess energy from the microenvironment surrounding the probe molecules, is operating in the hybrid compounds. To obtain deeper insight into the dam-effect of heat transfer in the hybrid environment, an observation of "hot bands" in highly vibrationally excited states and their relaxation by means of time resolved vibrational spectroscopy shall be investigated in the near future.[39]

One of the interesting points observed here is the two-component decay with τ_1 and τ_2 for both emissions of the probe molecules. It strongly suggests that both RhB and Rubpy situate at two different sites in the interlayer of the hybrid compounds as the τ_1 species (Species 1) and τ_2 one (Species 2). For example, the temperature gradient among Species 1 (104 °C for RhB) and 2 (47 °C for RhB) in RhB/**C3F-Azo-C6H**/SSA could be attributed to the different sites of incorporation of the dye molecule within the microenvironment (Table 1). As we have previously observed in nanosecond laser flash photolysis of **C3F-Azo-C6H**/SSA, the trapped thermal energy was supposed to be dissipated *via* three steps: initially within the central bilayer space of the interlayer sandwiched by perfluoroalkyl layers a large local temperature elevation was induced within $\sim$130 ns, then the slowly-cooling down temperature gradually propagated towards the clay nano-sheets ($\sim$1.4 μs), and finally the heat dissipation to surrounding media followed by thermodynamic equilibration ($\sim$8 μs).[23] Here Species 1 (τ_1) of both RhB and Rubpy that suffer the higher temperature could be assigned to be situated at the central space sandwiched by perfluoroalkyl layers, and Species 2 (τ_2) could attach to the surface of the clay nano-sheets to experience the lower temperature elevation (Fig. 8). Another crucial point should be that the higher temperatures of both species (τ_1 and τ_2) in the microenvironment of **C3F-Azo-C6H**/SSA compared to **C3H-Azo-C6H**/SSA demonstrates the retardational effect of perfluoroalkyl layers
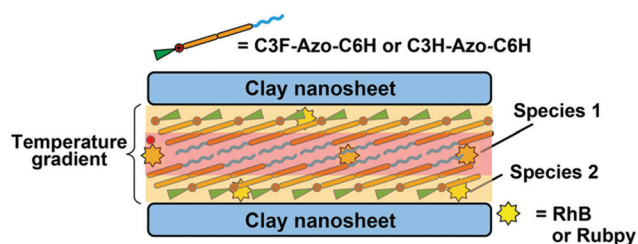
that have inherently very weak intermolecular interactions, causing such insensitivity to the propagation of energy dissipation as expected (Tables 1 and 2). All these results strongly support thermal energy trapping within the layered microenvironment, which rationalizes the previously observed and unusually high quantum yield of photo-isomerization,[21] as well as the transient behaviour in the nanosecond laser flash photolysis experiments.[11] Such unusual heat-trapping within the nano-layered microenvironment would lead to temperature elevation and cause the three-dimensional morphological motion of the hybrid compounds (Fig. 2).[18,19,22,24]

3. Experimental

Materials

The synthetic silicate layered host material – SSA, was purchased from Kunimine Industries Co. Ltd. The two guest material cationic azobenzene surfactant molecules – with polyfluorinated chain (**C3F-Azo-C6H**) as well as the corresponding hydrocarbon analogue (**C3H-Azo-C6H**) – were originally synthesized by our group.[19,20] RhB and Rubpy were purchased from the Tokyo Chemical Industry Co., Ltd. (TCI). Ethanol (99%, Shinwa Alcohol Industry Co., Ltd) and ion-exchanged water (specific resistance <0.1 μS cm^{-1}) were used as solvents.

Sample preparation and characterization

An aqueous mixture of SSA (10^{-3} eq. L^{-1}) was prepared by dissolving 1 g of SSA in 1 L of water with stirring for one day. Along with that, an aqueous solution of **C3F-Azo-C6H** (5 mM) was prepared by heating at 70 °C for 5 hours in water and an aqueous solution of RhB (0.1 mM) was also prepared. The three samples in a volumetric ratio were mixed thoroughly, heated and stirred at 70 °C in an oil bath for 5 h to form the RhB/**C3F-Azo-C6H**/SSA hybrid. Loading levels of RhB were adjusted by changing the concentration of the dye solution. The hybrid mixture prepared above was filtered with 0.1 μm PTFE membrane and then the precipitate layer was attached and the membrane filter was placed on a cleaned glass plate. The membrane filter paper was carefully peeled off from the precipitate layer film. The film samples were then dried under vacuum and characterized using XRD, UV-vis and emission spectroscopy. Similarly, the 1% RhB/**C3H-Azo-C6H**/SSA co-intercalated hybrid was also prepared and characterized to study the effect of the polyfluorinated structure in the microenvironment.

Rubpy co-intercalated hybrid samples were prepared similarly to RhB intercalation using 0.1 mM Rubpy in water and then dried under vacuum, followed by characterization using XRD, UV-vis and emission spectroscopy.

XRD measurements were carried out using Rigaku (RINT TTR III). Thermogravimetric/differential thermal analysis measurements were carried out using a Shimadzu DTG-60H. An Nd:YAG laser-pumped OPG (EKSPLA, PL2210JE + PG432-JE; FWHM 26 ps, 1 kHz, 0.25 μJ mm^{-2}) was used as the excitation source for measuring the emission lifetimes in various

Fig. 8 Schematic representation of temperature gradient formation in the microenvironment of the dye/surfactant/SSA hybrid.

This journal is © the Owner Societies 2020

Phys. Chem. Chem. Phys., 2020, **22**, 7201–7209 | **7207**

microenvironments under the single photon counting condition of a streak camera (Hamamatsu photonics, C4334).

4. Conclusions

Two dye molecules, RhB and Rubpy, that can be used as temperature probing molecules by means of their temperature dependent emission lifetimes, were each successfully co-intercalated into surfactant/clay (**C3F-Azo-C6H**/SSA and **C3H-Azo-C6H**/SSA) interlayers in trace amounts. In various microenvironments including water, micelles, and the surfactant/clay, excited state emission lifetimes were measured to estimate quantitatively the transient temperature elevation occurring in the hybrid nano-layered environment. The two component decay of emission in each system of RhB and Rubpy indicated an existing temperature gradient in the microenvironment of the surfactant/clay systems. The transient temperature rise of 10–120 °C could be assigned to those in the bi-layered region within the interlayer space, and 40–60 °C to those near the inner surface of the layered clay. Moreover, the perfluoroalkyl chain layer was found to evidently dam the trapped heat to retard its dissipation. All this strongly supports thermal energy trapping within the layered microenvironment, which rationalizes the previously observed unusually high quantum yield of photo-isomerization as well as the transient behaviour in the nanosecond laser flash photolysis experiments. Such unusual heat-trapping within the nano-layered microenvironment would lead to temperature elevation and cause the three-dimensional morphological motion of the hybrid compounds.

Conflicts of interest

There are no conflicts to declare.

Acknowledgements

Notes and references

1 J.-M. Lehn, *Science*, 1993, **260**, 1762–1764.
2 J.-M. Lehn, *Supramolecular Chemistry: Concepts and Perspectives*, VCH, Weinheim, 1995.
3 Y. Hori, H. Ueno, S. Mizukami and K. Kikuchi, *J. Am. Chem. Soc.*, 2009, **131**, 16610–16611.
4 W. Szymański, J. M. Beierle, H. A. V. Kistemaker, W. A. Velema and B. L. Feringa, *Chem. Rev.*, 2013, **113**, 6114–6178.
5 S. Tadepalli, J. M. Slocik, M. K. Gupta, R. R. Naik and S. Singamaneni, *Chem. Rev.*, 2017, **117**, 12705–12763.
6 Y. Kameo, S. Takahashi, M. Krieg-Kowald, T. Ohmachi, S. Takagi and H. Inoue, *J. Phys. Chem. B*, 1999, **103**, 9562–9568.
7 M. Nagashima, T. Tsukamoto, T. Shimada, D. A. Tryk, S. Takagi and H. Inoue, *Bull. Chem. Soc. Jpn.*, 2014, **87**, 1273–1277.
8 H. Kusaka, M. Uno, M. Krieg-Kowald, T. Ohmachi, S. Kidokoro, T. Yui, S. Takagi and H. Inoue, *Phys. Chem. Chem. Phys.*, 1999, **1**, 3135–3140.
9 T. Yui, H. Yoshida, H. Tachibana, D. A. Tryk and H. Inoue, *Langmuir*, 2002, **18**, 891–896.
10 T. Yui, S. Fujii, K. Matsubara, R. Sasai, H. Tachibana, H. Yoshida, K. Takagi and H. Inoue, *Langmuir*, 2013, **29**, 10705–10712.
11 T. Yui, K. Takagi and H. Inoue, *J. Photochem. Photobiol., A, Chem.*, 2018, **363**, 61–67.
12 C. W. Lawson, F. Hirayama and S. Lipsky, *J. Chem. Phys.*, 1969, **51**, 1590–1597.
13 R. E. Banks, *Organofluorine Chemicals and their Industrial Applications*, Ellis Horwood Ltd, Chichester, UK, 1979.
14 T. Kitazumi, T. Ishihara and T. Taguchi, *Chemistry of Fluorine*, Kodansha Scientific, Tokyo, 1993.
15 A. Negishi, *Chemistry of Fluorine*, Mruzen, Tokyo, 1988.
16 Z. Tong, S. Takagi, T. Shimada, H. Tachibana and H. Inoue, *J. Am. Chem. Soc.*, 2006, **128**, 684–685.
17 Z. Tong, S. Sasamoto, T. Shimada, S. Takagi, H. Tachibana, X. Zhang, D. A. Tryk and H. Inoue, *J. Mater. Chem.*, 2008, **18**, 4641–4645.
18 Y. Nabetani, H. Takamura, Y. Hayasaka, T. Shimada, S. Takagi, H. Tachibana, D. Masui, Z. Tong and H. Inoue, *J. Am. Chem. Soc.*, 2011, **133**, 17130–17133.
19 Y. Nabetani, H. Takamura, Y. Hayasaka, S. Sasamoto, Y. Tanamura, T. Shimada, D. Masui, S. Takagi, H. Tachibana and Z. Tong, *Nanoscale*, 2013, **5**, 3182–3193.
20 V. Ramakrishnan, D. Yamamoto, S. Sasamoto, T. Shimada, Y. Nabetani, H. Tachibana and H. Inoue, *Phys. Chem. Chem. Phys.*, 2014, **16**, 23663–23670.
21 Y. Nabetani, A. Uchikoshi, S. Miyajima, S. Z. Hassan, V. Ramakrishnan, H. Tachibana, M. Yamato and H. Inoue, *Phys. Chem. Chem. Phys.*, 2016, **18**, 12108–12114.
22 Y. Nabetani, H. Takamura, A. Uchikoshi, S. Z. Hassan, T. Shimada, S. Takagi, H. Tachibana, D. Masui, Z. Tong and H. Inoue, *Nanoscale*, 2016, **8**, 12289–12293.
23 V. Ramakrishnan, Y. Nabetani, D. Yamamoto, T. Shimada, H. Tachibana and H. Inoue, *Phys. Chem. Chem. Phys.*, 2017, **19**, 4734–4740.
24 S. Z. Hassan, Y. Nabetani, A. Matsumoto, T. Shiragami, Z. Tong, H. Tachibana and H. Inoue, *Phys. Chem. Chem. Phys.*, 2019, **21**, 21738–21745.
25 M. Snare, F. Treloar, K. Ghiggino and P. Thistlethwaite, *J. Photochem.*, 1982, **18**, 335–346.
26 K. Kemnitz, N. Nakashima, K. Yoshihara and H. Matsunami, *J. Phys. Chem.*, 1989, **93**, 6704–6710.
27 N. Kitamura, Y. Hosoda, C. Iwasaki, K. Ueno and H.-B. Kim, *Langmuir*, 2003, **19**, 8484–8489.
28 K. Yao, S. Nishimura, Y. Imai, H. Wang, T. Ma, E. Abe, H. Tateyama and A. Yamagishi, *Langmuir*, 2003, **19**, 321–325.
29 T. Kajiwara, K. Hashimoto, T. Kawai and T. Sakata, *J. Phys. Chem.*, 1982, **86**, 4516–4522.

7208 | *Phys. Chem. Chem. Phys.*, 2020, **22**, 7201–7209

This journal is © the Owner Societies 2020

30 R. S. Lumpkin, E. M. Kober, L. A. Worl, Z. Murtaza and T. J. Meyer, *J. Phys. Chem.*, 1990, **94**, 239–243.

31 M. K. Brennaman, J. H. Alstrum-Acevedo, C. N. Fleming, P. Jang, T. J. Meyer and J. M. Papanikolas, *J. Am. Chem. Soc.*, 2002, **124**, 15094–15098.

32 H.-B. Kim, N. Kitamura and S. Tazuke, *Chem. Phys. Lett.*, 1988, **143**, 77–80.

33 R. W. Ramette and E. B. Sandell, *J. Am. Chem. Soc.*, 1956, **78**, 4872–4878.

34 H. Watarai and F. Funaki, *Langmuir*, 1996, **12**, 6717–6720.

35 D. Setiawan, A. Kazaryan, M. A. Martoprawiro and M. Filatov, *Phys. Chem. Chem. Phys.*, 2010, **12**, 11238–11244.

36 A. L. Smirl, J. B. Clark, E. W. Van Stryland and B. R. Russell, *J. Chem. Phys.*, 1982, **77**, 631.

37 J. B. Birks and L. G. Christophorou, *Photophysics of Aromatic Molecules*, John Wiley & Sons Ltd., 1969.

38 S. Rafiq and G. D. Scholes, *J. Phys. Chem. A*, 2016, **120**, 6792–6799.

39 T. Mukuta, S. Tanaka, A. Inagaki, S. Koshihara and K. Onda, *ChemistrySelect*, 2016, **1**, 2802–2807.